

WIDN

3725-00015

An aerial Synthetic Aperture Radar (SAR) image of a landscape. The terrain is textured with various shades of green and blue, indicating different surface features. Two prominent bright spots are visible: a large, irregularly shaped bright area in the upper center, and a smaller, more circular bright spot in the lower right. The bright spots likely represent areas of high reflectivity, possibly due to water or other surface characteristics.

The use of DInSAR for aquifer pumping analysis

**Michael Widmer
Satellite Radar Imaging
Geol 702h
Spring 2005**

INTRODUCTION

Satellite radar is the technique of impinging a coherent microwave upon the earth's surface and examining its reflected energy at the receiving antenna. This energy is measured in terms of the reflected wavelength's amplitude and phase, and compared to the original transmitted microwave. Satellite radar found its initial usefulness in the identification and measurement of landforms such as in geomorphology and topography. These techniques were largely based upon the amplitude of the reflected microwave. In the last ten to twelve years, differential interferometry, using synthetic aperture radar (InSAR), has found success in the measurement of ground surface deformation. This technique investigates any differences in land surface displacements during the time span between two or more satellite scenes. Land surface displacements, given the same precise geographic location, can be determined by measuring any difference in the reflected microwave phase. The precision of this technique becomes a function of the measurement of microwave phase change and not through the direct measurement of topography (Zebker et al., 1992). As a result, displacements can be measured at the sub-centimeter scale. These types of surface displacements can determine both horizontal and vertical motion.

This technique is now commonly applied to earthquake-fault displacement and volcanic activity, among other uses. Additional work has proven this technique's usefulness in examining land subsidence due to ground water withdrawals (ref). Land subsidence will occur when the volume and extent of groundwater depletion exceeds the aquifer's elasticity. This elasticity is supported by the aquifer's structural framework made up of both granular media, air and water. Aquifer elasticity does allow for "land surface flexure" given appropriate changes in the volumetric water and air content.

This paper presents evidence for the measurement of land surface flexure using differential interferometry (DInSAR). These slight changes in land elevations can be due to changes in the volume of groundwater in regional aquifers (aquifer elasticity). These volumetric changes are due to well field production (ground water extraction) and the spatial rate and timing of ground water recharge. Of particular note will be the comparison of DInSAR anomalies to well field production using a "production influence function" similar to the Mogi Source Function for subsurface volume displacement. This paper will also discuss other ground water related trends in InSAR anomalies presented such as porosity, permeability, faults, lag time of aquifer trends and land effects. Tectonic changes are probably measurable in the same time frame and to the same degree of precision, but for this investigation are not considered.

Acknowledgements

The author would like to acknowledge the Western North American Interferometric Satellite Radar Consortium for the acquisition of satellite radar images and processing software, my mentor Dr. Gary Oppliger, fellow colleague Justin Huntington, and the data and resources provided by Washoe County, Truckee Meadows Water Authority, and the University of Nevada.

STUDY AREA

The Truckee Meadows (Figure 1) is located in central western Nevada at the California border. It is also located at the base of the Sierra Nevada and the western fringe of the Basin and Range Province and therefore surrounded by 8,000 to 10,000 feet mountain ranges. This 150mi² geographic area lies within a basin, of normal strike-slip fault structure, and bordered by alluvial fans, pediments and terraced bluffs. This semi-arid, high desert region (elevation 4400 feet) receives precipitation due to orographic and rain shadow effects and varies from 6in in the center of the basin, 22in near the mountain fronts and up to 60in. within the Carson Range of the Sierra Nevada (Kleiforth, 1983). Precipitation mostly occurs in the winter months whereby 75% of the annual precipitation is realized. Summers are mostly clear of clouds except for abundant cumulous nimbus activity. Mountain streams emanate from the Sierra Nevada and form the Truckee River that largely flows from Lake Tahoe and historically discharged into Pyramid Lake. The Truckee Meadows are the geomorphic result that, pre-industrial man, consisted of lakes, meadows and wetlands.

Today, the cities of Reno and Sparks and Washoe County are experiencing rapid metropolitan growth despite limited land and water resources. Two major public water supply purveyors provide service to the area, the Truckee Meadows Water Authority (TMWA) and the Washoe County Department of Water Resources (WCDWR). Both public agencies operate water production well fields, TMWA in the Central Truckee Meadows (CTM) and WCDWR in the South Truckee Meadows (STM). TMWA largely draws upon the Truckee River to meet its average day demands for water supply. TMWA supplements this surface water source with ground water where its well field is mostly in use during May through September. The WCDWR's well field is the major water supply source with minor augmentation from the TMWA's system. Figure 1 shows the location of these well fields where "P" indicates a TMWA production well and WC indicates WCDWR production well. Annual groundwater pumpage is approximately 17,000af and 5,000af, respectively.

PRODUCTION INFLUENCE FUNCTION

What is the purpose of applying this function to well field production?

Typically, monitor wells are used to measure and observe changes in water levels in the aquifer due to rates of change in recharge and discharge. These are point measurements and tens to hundreds of these wells and subsequent measurements are needed to adequately observe aquifer pressure changes on a regional scale. Regional aquifer response to large scale pumping is typically assessed with numerical simulation models of the aquifer. These methods demand substantial resource investments. Another method, explored in this paper, is the use of the Mogi Source Function (Mogi, 1958). This function is used to estimate the effect of volume displacement at a radial distance from a subsurface source adding or extracting mass. Oppliger (2005) has adapted this function for groundwater production well fields and its cumulative effects of groundwater withdrawal, referred to as the Production Influence Function (PIF) in equation 1.

$$dy = Q * D * (\text{conv}/2\pi) / (l\text{sr})^3 \quad (1)$$

where:

Q = production in acre-feet

D = scaling factor with range centered at 1000m; $\times 10^{+/-1}$

conv = 4047 m²/acre-feet

lsr = $(\text{SQRT } X^2 + Y^2 + D^2)^3$

This function should not be construed as a measurement of ground water depletion. It is a scaling tool of the cumulative, volumetric displacement of fluid withdrawal. The use of the function is justified in illustrating the spatial impact of fluid withdrawals. This function will be applied to the time specific groundwater pumpage and compared to DInSAR anomalies within the Truckee Meadows.

The function is applied in the following way. The study area was gridded into 200m cells. Each production well was geo-referenced to this grid such that each cell was calculated for the production influence based upon the production volume. The influence, measured in feet, that a production well influences will be a function of the distance from the cell to the well. After all production well influences are calculated for all cells, a summation of the different influences for each cell is made and then gridded (minimum curvature). This grid is then contoured and displayed atop InSAR images as are the production well locations for analysis.

Production well data

Table 1 lists the annual pumpage, in million gallons, that were produced from the respective wellfields. The pumpage from TMWA varied between 2,500 and 5,100 mg over the 1990s and average 4,100 mg. WCDWR pumpage mostly increased its annual pumpage from 400 mg to 1,300 mg. Also, precipitation averages are listed in the table as the percent of normal measured at the Reno Airport precipitation gauge (WRCC, 2005).

Table 1
Production wellfield pumpage
(million gallons)

| Year | TMWA | WCDWR | % normal precipitation |
|------|-------|-------|------------------------|
| 1990 | 4,743 | 420 | 72 |
| 1991 | 4,712 | 408 | 70 |
| 1992 | 5,114 | 523 | 73 |
| 1993 | 3,092 | 472 | 90 |
| 1994 | 5,125 | 651 | 71 |
| 1995 | 4,796 | 635 | 172 |
| 1996 | 4,115 | 770 | 167 |
| 1997 | 2,560 | 920 | 106 |
| 1998 | 2,523 | 914 | 165 |
| 1999 | 3,830 | 1,308 | 60 |

The largest producing wells for TMWA (see Figure 1) are P22, P29, P13 and P16. The largest producing wells for WCDWR are WC 22, WC17 and WC18.

DIFFERENTIAL INTERFEROGRAMS

Differential Interferometric Synthetic Aperture Radar is a technique whereby two geo-referenced satellite scenes are digitally compared to examine any change in microwave phase from the exact same resolution cells (20m pixels). Changes in phase, with coherent data, will be due to land surface displacement in the resolution cell itself. For example the effects of tectonic movement or subsidence can be imaged in this manner, within limitations. These limitations are usually dictated by temporal (land use changes or vegetative growth) and baseline (satellite orbits and tracks) correlation between the two images.

Single Look Complexes

Satellite radar scenes, as Single Look Complexes (SLC), were purchased from the Western North American Interferometric Synthetic Aperture Radar Consortium (<http://www.winsar.scec.org/>). The data were acquired by the European Space Agencies ERS 1 and 2 satellites (Track 256, Frame 2817). These satellites transmit a 5.6cm coherent wavelength with horizontal polarization.

Three SLC were used for this investigation. Interferogram pairs 5 and 16 were formed using SLC 11/30/93 and 10/19/95, and SLC 03/30/03 and 11/30/93, respectively. Perpendicular baselines of Pair 5 are -65m and -41m and Pair 16 are -322m and -65m. These baselines are in reference to the first acquired SLC dated 04/14/92. The effective perpendicular baselines are 24m and 257m, respectively, well within the acceptable range for differential interferometry, particularly Pair 5. The focus processing, using ROI_PAC software (JPL, 19xx), of the SLC included:

1. assurances of correlation,
2. corrections for satellite orbit effects,
3. 4-looks filtering,
4. removal of topography (90m DEM),
5. power spectral density filtering,
6. removal of any prevalent banding,
7. geo-coded, and
8. unwrapped.

Once the interferograms were formed, additional processing by Dr. Oppliger converted the observed phase changes to a vertical displacement field.

Interferograms

Figure 2 is the interferogram for Pair 5 (November 30, 1993 to October 19, 1995) shown for the Truckee Meadows. In the northern half of the Figure, deflation in the land surface occurs over two distinct areas. Deflation of up to 20mm is found in the Central Truckee Meadows and up to 10mm in the northwestern portion of the Figure. Small areas of inflation can be found of up to 10mm. Also of interest is the anomaly located in the southern portion of the Figure where deflation of 30mm or more is shown. This anomaly is centered over the Steamboat Springs Geothermal Area, but will not be discussed in this report.

Figure 3 shows the interferogram of Pair 16 (March 30 to November 30, 1993). In this Figure, inflation up to 20mm, is shown to occur over most of the Central Truckee Meadows. Conversely, up to 10mm of deflation is shown to have occurred on the Mt. Rose Pediment and the Steamboat Hills of the South Truckee Meadows. There appears to be a linear boundary, from southeast to northwest, between the areas of deflation and inflation.

RESULTS

Figure 4 displays the Pair 5 Interferogram. Overlain is the gridded and contoured (0.5 feet interval) Production Influence Function (PIF) as applied to the TMWA production well field (red dots). Very good, apparent correlation is shown. As discussed above, the influence of the production volumes per individual well are assigned to a 200m grid spanning the area. Values of the PIF range from 0 to 3.5ft. The highest influence values are centered at the highest producing wells, P29 and P22. It appears in this interferogram that the use of the PIF infers a physically based correlation. The value of D, the lateral shaping coefficient, is 1000m.

Figure 5 displays the Pair 16 Interferogram with both the TMWA and WCDWR well fields and their volumetric production influence. Also shown is the course of the Truckee River. Recall that the interferogram shows large broad areas of inflation (20mm) and deflation (10mm). In viewing this Figure it must be noted that a 50% reduction in the lateral shaping coefficient, D, is used (500m). This gave better definition of the PIF than using 1000m.

The contoured plots of the PIF in the TMWA well field are much smaller than the previous interferogram, but still show as much as 2ft of influence at two well sites (P22 and WC5/6). The western and central fields are separate in this interferogram. The PIF as applied to the WCDWR well field in the STM shows as much as 1ft of influence at most of their wells. However, there is poor correlation with respect to the PIF contours and the size of the deflation that covers the entire pediment, the Galena alluvial fan and, oddly, the Steamboat Hills. The location of wells does not exactly plot in the center of the PIF contours and is probably the result of using slightly different coordinates for the well plots versus the PIF.

Figure 6 re-displays the Pair 16 Interferogram against the WCWRD well field in the STM. Contoured (1 foot interval) is a change in water levels from a monitor well data set (67 wells) where end points are coincident with the Interferogram dates. Four feet of water level decline is estimated and centered on well WC17, the largest producer in the STM. A water level rise can be seen in the southwest portion of the Figure, sandwiched between two and three feet declines. This may be due to domestic pumping or the gridding algorithm. In the area to the north of the well field, water levels rise to as much as four feet during the eight month time period.

DISCUSSION

As stated above, the summation of the production influences and the well locations are centered on the dInSAR deflation anomalies displayed in Figure 4. The PIF results are

based upon the production volumes of the well field and not the physical character of the aquifer. However, aquifer characteristics should correlate to the dInSAR anomalies in that the magnitude of the anomaly is a reflection to the type of aquifer material, the porosity and consequent permeability. These characteristics can describe the "elasticity" of an aquifer, particularly confined aquifers.

World-wide examples of major land subsidence due to ground water pumping occurs where fine grain sediments make up the aquifer material. In confined aquifers, the aquifer sediments, or grains, provide the skeletal structure that supports the land surface. Water also adds structure to the aquifer. When this water is extracted, there will be some vertical, and horizontal, shrinkage of the aquifer. The opposite is also true of ground water recharge events that can cause the aquifer to expand. This phenomena is manifested at the land surface by vertical flexure, and in the aquifer as elasticity. Coarse-grained aquifers will have less elasticity due to its less flexible horizontal movement, the individual grains have greater mass and require more force to move. So it should come as no surprise that there is good correlation from well field pumping and the dInSAR anomaly in this area.

The contours depicted in Figure 4 represent a scaling factor of the summation of individual well pumpage influence in a lateral dimension. The Mogi Function is the proper function to apply in this example as it is a good tool to summarize fluid extraction. The physical coupling of the PIF, an adaptation of the Mogi Function, to fluid extraction can be accomplished with more analysis of these types of examples. The depth coefficient can be calibrated to production well screen. Also, the function can be related to the physical properties of the aquifer, but perhaps only with a calibration coefficient. Another physically based tool would be a radial fluid flow model, but at the expense of considerable resource and time.

Figure 5 presents an interesting example of both inflation and deflation of the land surface occurring under well fields. To explain this we have to review the antecedent precipitation events and those during the time span of the interferogram (March to November, 1993). Prior to the Spring of 1993, the region was experiencing a severe drought (by current standards). Below normal precipitation began in 1987 and continued through 1994. Precipitation at the Reno Airport was 70% of normal three years prior to 1993 and 90% of normal in 1993 (see Table 1). However, west of Reno, precipitation was well above normal (150% in Verdi) for the months of December and January indicating that significant snow melt recharge to aquifers was available. Also, the reservoirs in the Sierra that feed the Truckee River were augmented by those two months of above normal precipitation. As a result, the TMWA well field pumpage was almost minimal for the 1993 summer (see Table 1). Therefore, the impacts to the CTM aquifer were probably more in a recharge mode than discharge and consequently the aquifer expanded. The manifestation of this is seen in the dInSAR anomaly as inflation flexure. In the STM aquifer, deflated flexure is measured in the interferogram of 5mm to 10mm. Annual ground water pumpage had been increasing from 1984 through 1993 (see Table 1) and of course, the same drought was having its effect on this aquifer. Perhaps the previous wet winter had lesser effects as well. It is interesting to note that the deflation

covers a much greater area than the well field. The deflation covers all of the alluvial pediment and the Steamboat Hills. This should be analyzed more closely to see if there were any SLC processing errors or climatic conditions¹ that may have caused this anomaly.

Another data set to inspect is differences in ground water levels during the time span. Figure 6 is an attempt at this, but it is important that the water level measurements be coincident with the interferogram. The data set shown in Figure 6 was largely coincident and a trend of lower water levels is evident. The trends are not strikingly obvious. Only two wells of the seven show a drop in the piezometric surface and these only show a three and a four feet drop. This is probably not enough to cause the dInSAR anomaly particularly since the anomaly was so far wide spread. This suggests another physical process at work during this time frame.

The largest deflated area in the differential interferogram is centered west of the WC17 production well. This is interpreted, at this point, to be caused by the local fault structure. A regional, north-south striking fault has been proposed (Widmer, et al., 2005) that traverses the pediment directly to the east of the well. Therefore, ground water pumped from the well may have originated west of the well as the fault provides a barrier to ground water movement (Widmer, 1996).

Finally, much of the pediment and bajada of the pediment contain hundreds of domestic wells that influence the piezometric surface. The largest concentrations are found north and south of the WCDWR well field. Water level rises in this area could be cause, in part, by the decrease in pumping during October and November as seen in the interferogram.

CONCLUSIONS

From Figures 4, 5 and 6 it is apparent that the effects of ground water pumping can be imaged with satellite radar. Impacts to land surface flexure, as measured with InSAR for this study area, can be determined from pumping quantities of hundreds of acre-feet. The use of the Production Influence Function shows good promise as a tool for identifying the lateral extent of pumping as compared to differential interferograms. Providing an aquifer-physical basis of the Production Influence Function should continue as a second step. The depth coefficient should be tied to production well screen depths. The mathematics behind the Mogi Function are sound in this application (Oppliger, personal communication). More attention should be given to matching water level measurements with dInSAR anomalies. Extensive water level data for the CTM are available after 1999 and provide the level of detail required for more accurate cause and effect relationships to pumping and coincident dInSAR anomalies. Finally, dInSAR anomalies should be compared to ground water flow simulation models for further proof of the cause and effect of production wells.

¹ High humidity within the atmosphere will tend to slow down radar wavelengths with has the effect of prolonging the radar backscatter to the receiving satellite antenna and a consequent lengthening of the distance traveled. This would give the appearance of deflation if the conditions were prevalent during November 1993. However, the CTM inflation just a few miles north probably precludes this phenomena.

REFERENCES

- JPL, 19xx. Repeat Orbit Interferometry Package software. Jet Propulsion Laboratory, Pasadena, California.
- Kleiforth, H., Albright, E., Ashby, J. 1983. *Measurement, Tabulation and Analysis of Rain and Snowfall in the Truckee River Basin*. Atmospheric Sciences Center, Desert Research Institute Nevada, Reno. 99p.
- Mogi, K. 1958. *Relations between the eruptions of various volcanoes and the deformations of the ground surfaces around them*. Bull. Earthq. Res. Inst. Univ. Tokyo, 36, 99-134.
- Widmer, M., Oppliger, G., Henry, C., 2005. *A gravity-based structural analysis of Southern Washoe County, Nevada*. (in progress). Washoe County, University of Nevada and Nevada Bureau of Mines and Geology, Reno Nevada.
- Widmer, Michael. 1996. *Southwest Pointe Exploration and Well Construction Report*. Washoe County Department of Water Resources, Reno, Nevada.
- WRCC, 2005. Precipitation records on file with the Western Regional Climate Center, Desert Research Institute, Reno, Nevada.
- Zebker, H., Rosen, P., Goldstein, R., Gabriel, A., and Werner, C. 1994. *On the derivation of coseismic displacement fields using differential radar interferometry: The Landers earthquake*. Journal of Geophysical Research, Solid Earth. Vol. 99, no. 10, pp19617-19634.

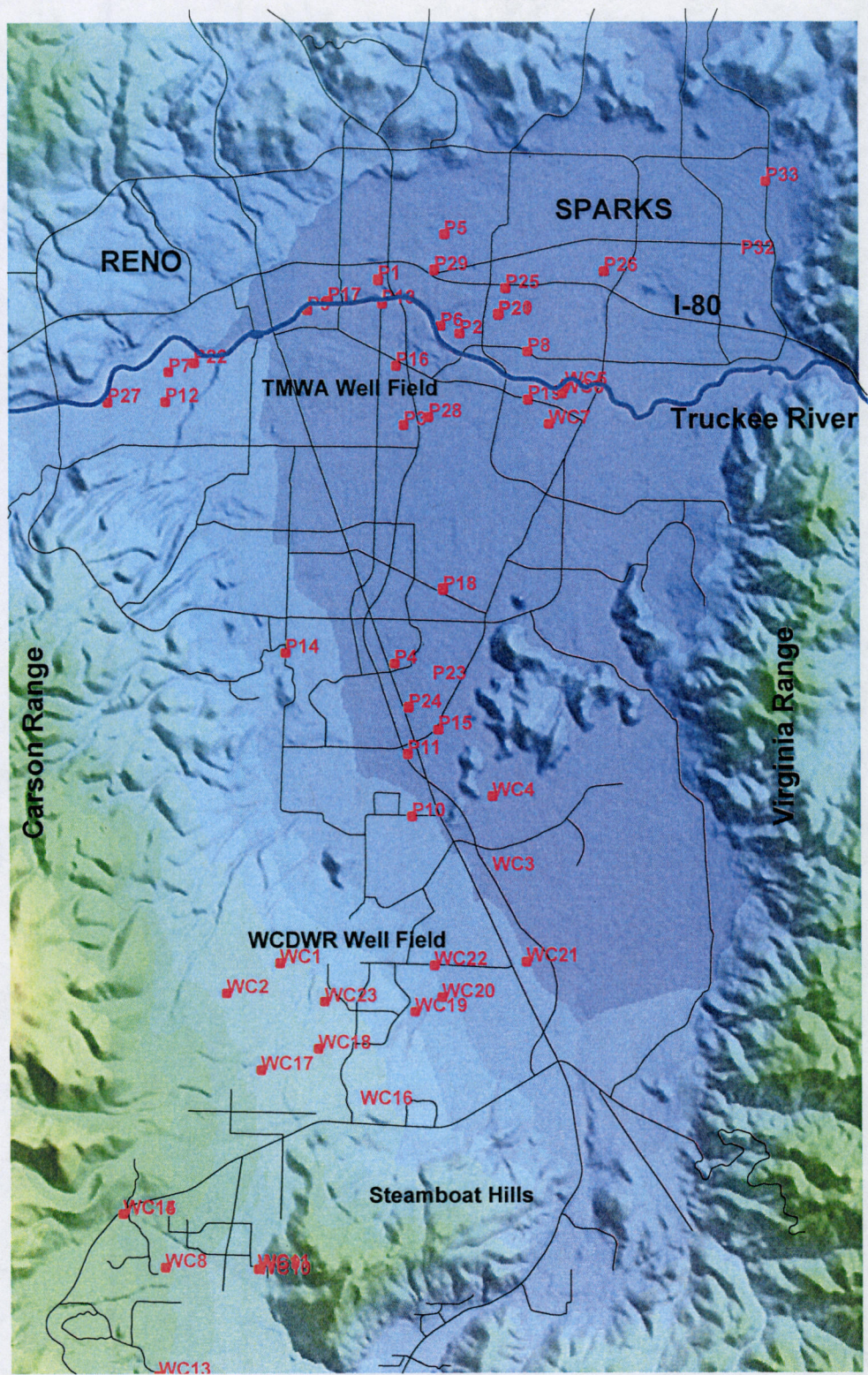
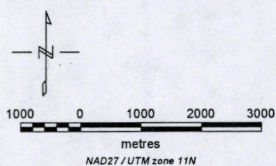


Figure 1. Truckee Meadows study area shown on color shaded relief map. TMWA and WCDWR wellfields are shown as of 1998.



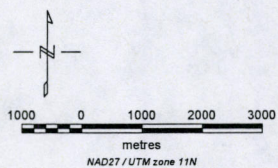
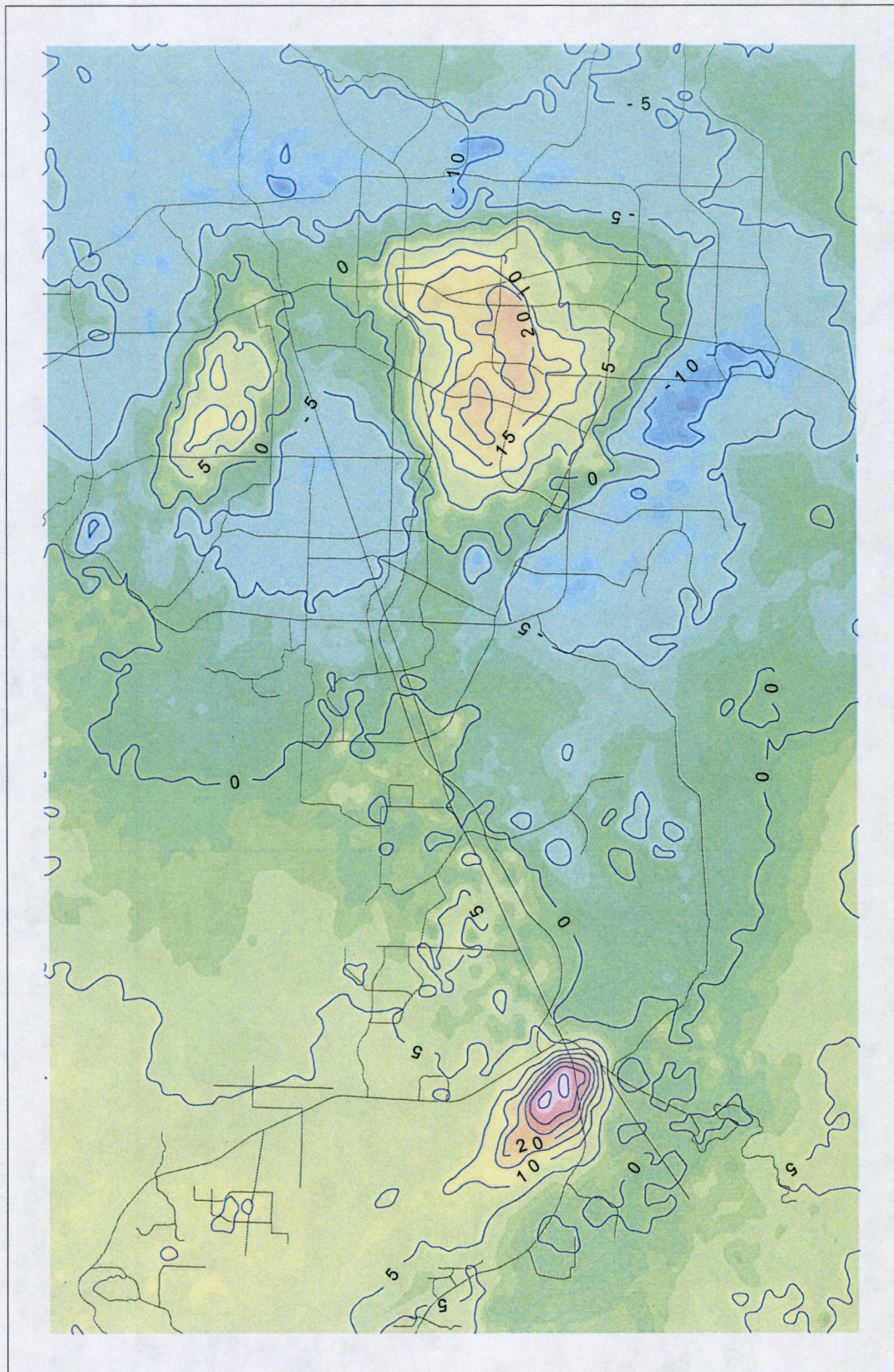


Figure 2. Pair 5 Interferogram processed for vertical displacement. Warm colors represent deflation of the ground surface. Contour interval is 5mm. Time frame spans 11/30/93 to 10/19/95

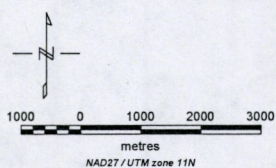
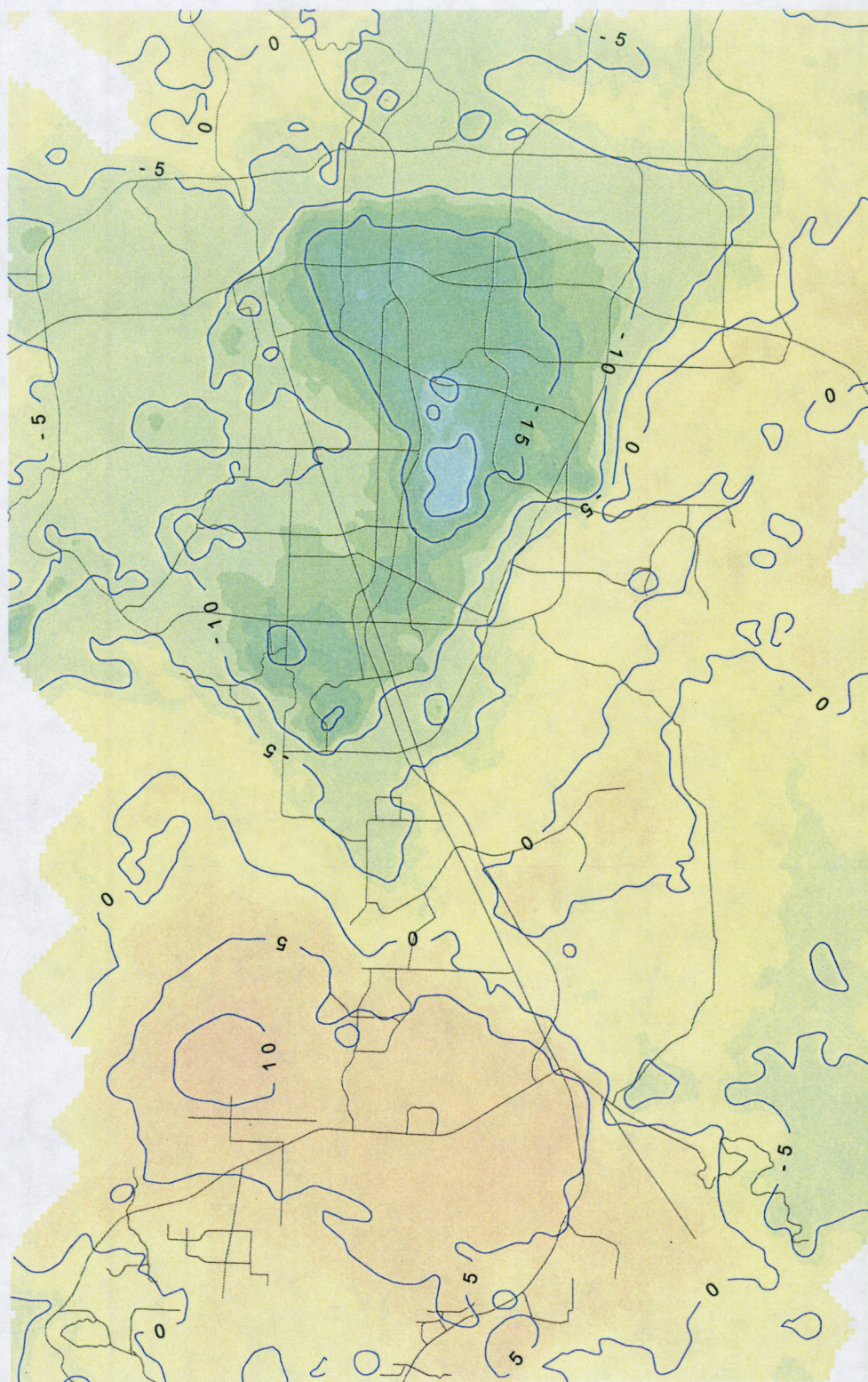


Figure 3. Pair 16 Interferogram processed for vertical displacement. Warm colors represent deflation of the ground surface, cool colors inflation. Contour interval is 5mm. Time frame spans 3/30/93 to 11/30/93.

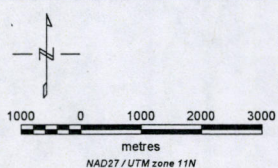
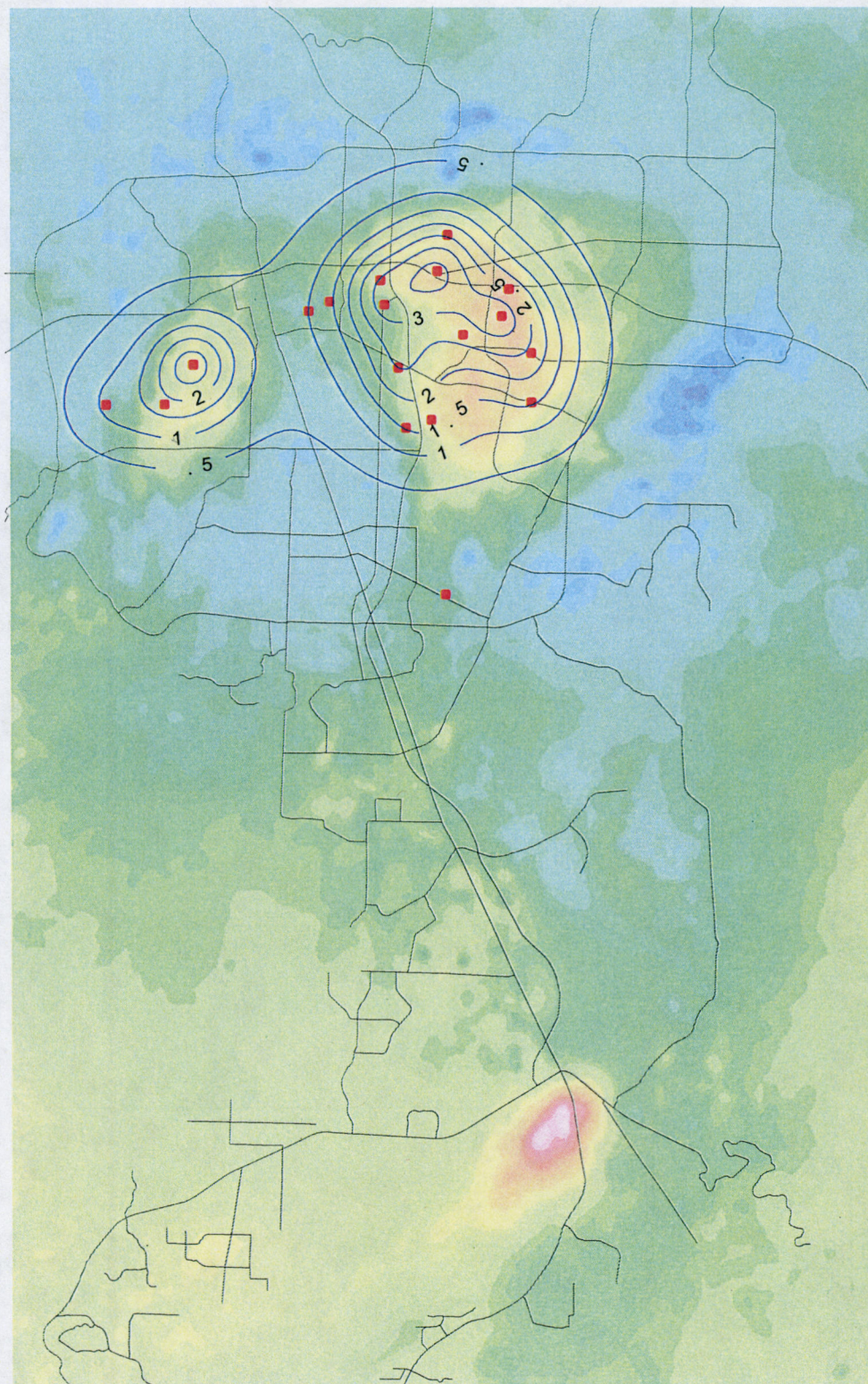


Figure 4. Pair 5 Interferogram with contour of Production Influence Function for TMWA wellfield. Contour interval is 0.5 feet. Maximum value is 3.5 feet. time frame spans 11/30/93 to 10/19/95

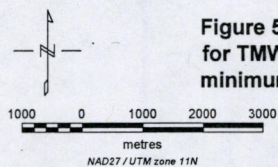
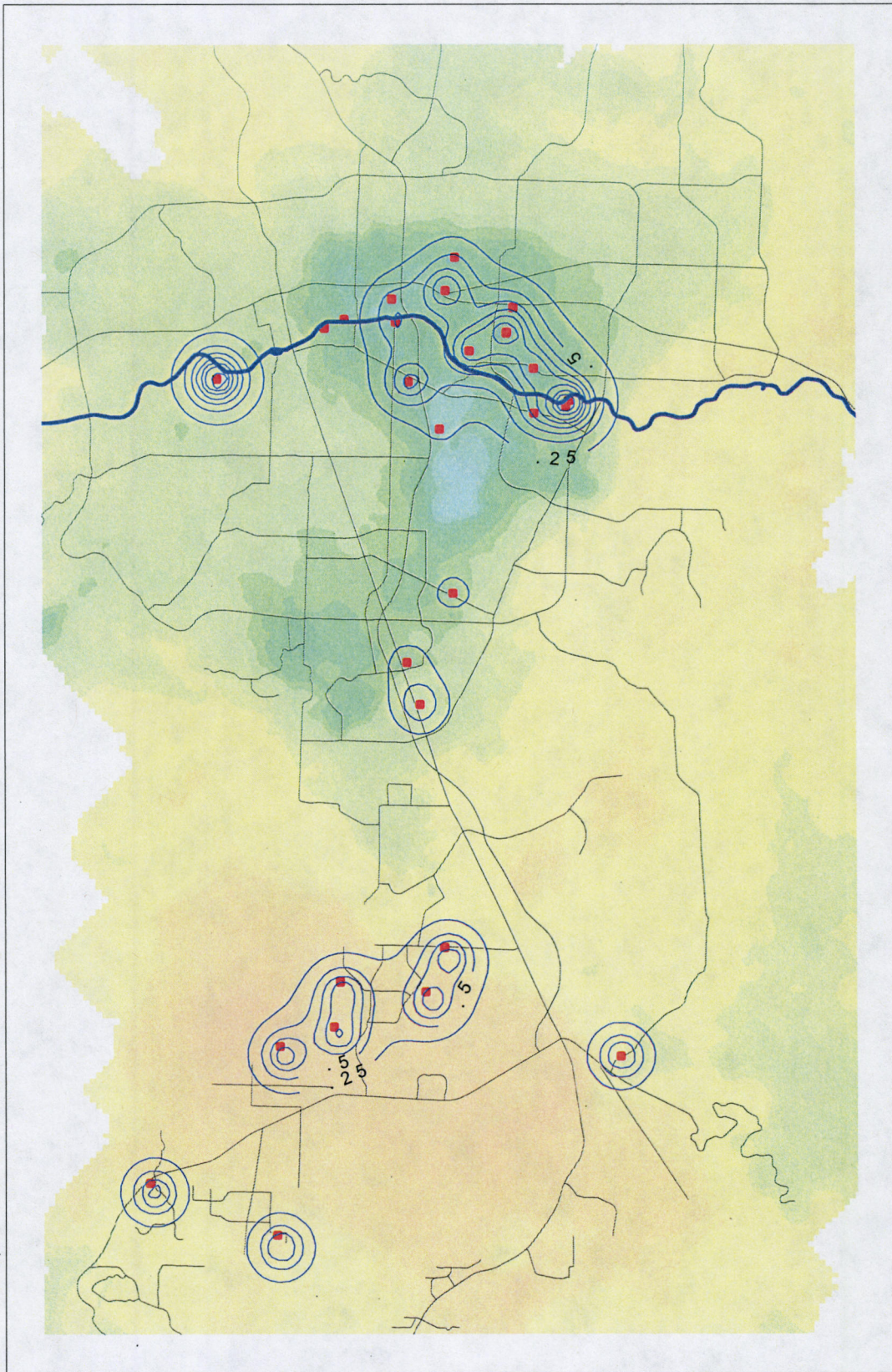


Figure 5. Pair 16 Interferogram with contour of Production Influence Function for TMWA and WCDWR well fields. Contour interval is 0.25 feet. Maximum and minimum values are 10mm and -20mm. Time frame spans 3/30/93 to 11/30/93.

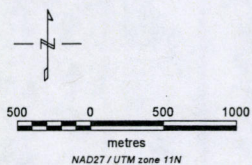
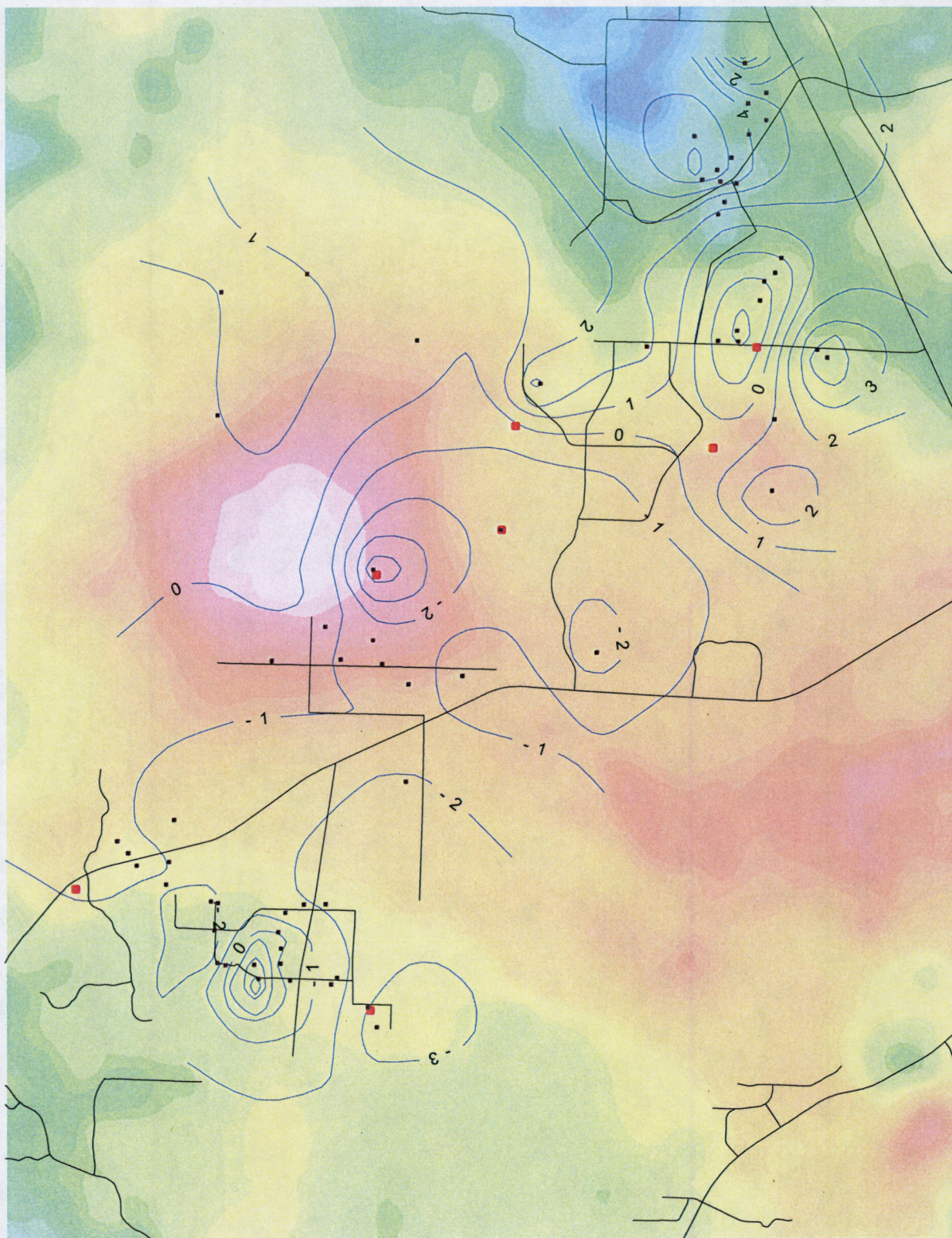


Figure 6. Water level changes during March to November, 1993 for Pair 16 Interferogram for the STM with monitor and production well locations for WCDWR. Contour interval is 1.0 feet. Color shaded relief highlighted from Figure 3.